DTP/98/80
November 1998

The Parton Content of Virtual Photons

M. Stratmann

Department of Physics, University of Durham,
Durham DH1 3LE, England

Abstract

The QCD treatment of the parton structure of virtual photons is briefly recalled, and possible limitations and open questions are pointed out. Various models for these densities are compared, completed by a short discussion of the treatment of heavy flavors. Finally, different ways to measure the parton distributions of virtual photons in e^+e^- and ep experiments are summed up.

Talk presented at the workshop on 'Photon Interactions and the Photon Structure', Lund, Sweden, September 1998.

The Parton Content of Virtual Photons

Marco Stratmann

Department of Physics, University of Durham, Durham DH1 3LE, England
E-mail: Marco.Stratmann@durham.ac.uk

Abstract

The QCD treatment of the parton structure of virtual photons is briefly recalled, and possible limitations and open questions are pointed out. Various models for these densities are compared, completed by a short discussion of the treatment of heavy flavors. Finally, different ways to measure the parton distributions of virtual photons in e^+e^- and ep experiments are summed up.

1 Introduction

Theoretical studies of photonic parton distributions of *real*, i.e., on-shell, photons have a long history initiated by Witten's work [1]. On the experimental side the past few years have seen much progress since the advent of HERA. The observation of 'resolved' photon induced ep processes, like (di-)jet photoproduction, allows for tests of the hadronic nature of (real) photons which are complementary to structure function measurements in e^+e^- collisions, where new results from LEP/LEP2 have improved our knowledge as well [2].

Studies of the transition of the (di-)jet cross section from the photoproduction to the deep-inelastic scattering (DIS) region at HERA point to the existence of a parton content also for *virtual* photons [3, 4]. These measurements have revived the theoretical interest in this subject and have triggered a series of analyses of the dependence of the ep jet production cross section on the virtuality of the exchanged photon [5, 6]. Recently, a next-to-leading order (NLO) QCD calculation of the (di-)jet rate in ep (and $e\gamma$) scattering, which properly includes the contributions due to resolved virtual photons, has become available [7, 8], and resolved virtual photons have been included for the first time also in the Monte Carlo event generator `RAPGAP` [9].

Pioneering work on the parton structure of virtual photons has been already performed a long time ago [10-12]. However, phenomenological models for these distributions have been proposed only in recent years [13-16] in view of the expected experimental progress. Ongoing measurements at HERA and future structure function measurements at LEP2 should seriously challenge these models and hopefully lead to a better understanding of the transition between the photoproduction and the DIS regime. To finish this introductory prelude, let us stress that photons provide us with a unique opportunity to investigate its parton content in a *continuous* range of masses (virtualities) in contrast to the situation with nucleons or pions.

The framework for parton distributions of virtual photons, theoretical expectations, and open questions are briefly recalled in Sec. 2. The various different models for the

parton content of virtual photons are compared in Sec. 3, supplemented by a short discussion of the treatment of heavy flavors in Sec. 4. In Sec. 5 we sum up the different ways to measure the parton densities of virtual photons in ep and e^+e^- experiments.

2 Theoretical framework: definitions, expectations, open questions

For clarity we henceforth denote the probed target photon with virtuality $P^2 = -p_\gamma^2$ by $\gamma(P^2)$, where p_γ is the four momentum of the photon emitted from, say, an electron in an e^+e^- or ep collider[1]. For real ($P^2 = 0$) photons we further simplify the notations by setting, as usual, $\gamma \equiv \gamma(P^2 = 0)$.

The concept of photon structure functions for real and virtual (*transverse*) photons can be defined and understood, in close analogy to deep-inelastic lepton-nucleon scattering, via the subprocess $\gamma^*(Q^2)\gamma(P^2) \to X$, as in $e^+e^- \to e^\pm X$ ('single tag') or $e^+e^- \to e^+e^-X$ ('double tag'). The relevant 'single tag' differential cross section can be expressed as in the hadronic case in terms of the common scaling variables x and y

$$\frac{d^2\sigma(e\gamma(P^2) \to eX)}{dxdy} = \frac{2\pi\alpha^2 S_{e\gamma}}{Q^4}\left[\left(1+(1-y)^2\right)F_2^{\gamma(P^2)}(x,Q^2) - y^2 F_L^{\gamma(P^2)}(x,Q^2)\right] \qquad (1)$$

with $F_{2,L}^{\gamma(P^2)}$ denoting the photonic structure functions. The measured e^+e^- cross section is obtained by convoluting (1) with the photon flux for the target photon $\gamma(P^2)$ [17]. The range of photon 'masses' (virtualities) produced is

$$m_e^2\, y^2/(1-y) \le P^2_{min} \le P^2 \le P^2_{max} \le \frac{S}{2}\,(1-y)(1-\cos\Theta_{max}) \ , \qquad (2)$$

where y is the energy fraction taken by the photon ($y = E_\gamma/E_e$), S is the available squared c.m.s. energy, and Θ_{max} is the maximal scattering angle of the electron in this frame. $P^2_{min,max}$ in (2) are further determined by detector specifications and/or an eventual tagging of the outgoing electron at the photon producing vertex. P^2_{min} effectively measures to a good approximation the dominant photon virtuality involved, just as $P^2_{min} = m_e^2 y/(1-y) \simeq 0$ represents quasi-real photons. Even in the latter case there is, however, still a small contribution from the high-P^2, virtual photon tail of the spectrum, which has to be estimated [16, 18] when one tries to extract the parton densities of real photons. For *transverse* virtual target photons $\gamma(P^2)$, whose virtuality P^2 is essentially given by $P^2 \simeq P^2_{min}$, one expects [10, 11] a parton content $f^{\gamma(P^2)}(x,Q^2)$ along similar lines as for real photons. The range of applicability of this 'picture', however, deserves a further scrutiny.

For real photons γ it is well-known that in the framework of the quark parton model (QPM) the x- and Q^2-dependence of $F_{2,L}^\gamma \equiv F_{2,L}^{\gamma(P^2)}$ is fully calculable from the 'pointlike' QED process $\gamma^*(Q^2)\gamma \to q\bar{q}$ if one introduces quark masses m_q to regulate the mass singularities due to $P^2 = 0$ [19]. However, this description is subject to perturbative QCD corrections due to gluon radiation not present in the QPM [1, 20]. The logarithmically

[1] In the latter case it is common to use $Q^2 = -q^2$ instead of P^2, but we prefer P^2 according to the original notation used in e^+e^- annihilations [10, 11], where it refers to the virtuality of the probed (virtual) target photon, and Q^2 is reserved for the highly virtual probe photon $\gamma^*(Q^2)$, $Q^2 = -q^2 \gg P^2$.

enhanced contributions $\alpha_s \ln Q^2/Q_0^2$ can be resummed to all orders, removing the dependence on effective quark masses, where Q_0 denotes some a priori *not* fixed renormalization point somewhere in the perturbative region $Q_0 \gg \Lambda_{QCD}$. Of course, this is not the whole story, since the photon can undergo a transition into a vector meson of the same quantum numbers, which is afterwards probed by the $\gamma^*(Q^2)$ (Vector Meson Dominance (VMD) assumption). This *non*-perturbative part obeys the same evolution equations as known from the hadronic case.

Turning to *virtual* photons, i.e., $P^2 \neq 0$, it is *expected* [10, 11] that for large enough virtualities P^2 one ends up with a *fully perturbative* prediction irrespective of Q^2. To facilitate the discussions, it is useful to define the relevant different ranges of P^2:

$$\begin{aligned} &\text{(I)} \quad P^2 \ll \Lambda^2_{QCD} \ll Q^2 \quad , \quad \text{(II)} \quad P^2 \simeq \Lambda^2_{QCD} \quad , \\ &\text{(III)} \quad \Lambda^2_{QCD} \ll P^2 \ll Q^2 \quad , \quad \text{(IV)} \quad P^2 \simeq Q^2 \quad . \end{aligned}$$

Case (I) we have already discussed above, since it refers to a (quasi-)real photon with $P^2 \simeq 0$. In range (III) one can apply similar considerations as long as one restricts oneself to *transverse* virtual photons [10, 11], with the important distinction that P^2 is now within the perturbative domain and hence can serve to fix Q_0, i.e., $Q_0 = \mathcal{O}(\mathcal{P})$. This is the basis for the above mentioned conjecture of absolute predictability in this case, since any non-perturbative VMD-inspired contributions are expected to vanish like $(1/P^2)^2$ due to such a 'dipole' suppression factor in the vector meson 'propagator'.

Several questions have to be addressed: up to which values of P^2 (and x, Q^2) is the non-perturbative part relevant? What are the lower and upper bounds on P^2 in (III), i.e., where and how takes the transition to regions (II) and (IV), respectively, place, and down to which value of P^2 in (III) should one trust perturbation theory? For smaller P^2, i.e., for a transition to the parton content of real photons (I), one has to find some appropriate, physically motivated prescription which *smoothly* extrapolates through region (II), where perturbation theory cannot be applied, down to $P^2 = 0$. On the other side, P^2 is bounded from above by $P^2 \ll Q^2$ in order to avoid power-like (possibly higher twist) terms $(P^2/Q^2)^n$ which should spoil the dominance of the resummed logarithmic contributions $\sim \alpha_s \ln Q^2/P^2$ and, furthermore, to guarantee the dominance of the transverse photon contributions in physical cross sections. For P^2 approaching Q^2 (region (IV)) the e^+e^- result should reduce to the one given by the *full* fixed order box $\gamma^*(Q^2)\gamma(P^2) \to q\bar{q}$ including all $(P^2/Q^2)^n$ terms and possibly $\mathcal{O}(\alpha_s)$ QCD corrections, which are unfortunately unknown so far.

The question of when fixed order perturbation theory becomes the more reliable prescription and the concept of virtual transverse photonic parton distributions (i.e., resummations) becomes irrelevant and perhaps misleading is in some sense similar to the question of whether heavy quarks should be treated as massless partons or not, which was extensively discussed in the literature recently [21, 22]. Both issues are characterized by the appearance of at least two different, large scales, P^2 and Q^2 (or m_q^2 and Q^2), which might be indicative for resummations or not. In our case here, however, one is also interested in the transition to a region where resummations are indispensable (i.e., for real photons), but the range of applicability of this approach with respect to P^2 (and possibly x and Q^2) cannot be determined reliably so far unless the full NLO corrections to the $\gamma^*(Q^2)\gamma(P^2)$ box will be available to analyze its perturbative stability.

As already mentioned, for a given $Q^2 \gg P^2$ and increasing P^2 one expects that the resummed results approach the QPM result determined for $m_q^2 \ll P^2 \ll Q^2$, due to

the shrinkage of the evolution length, i.e., less gluon radiation. The QPM result can be obtained from the process $\gamma^*(Q^2)\gamma(P^2) \to q\bar{q}$, but now $P^2 \neq 0$ can act as the regulator and no quark masses have to be introduced. Taking the limit $P^2/Q^2 \to 0$ whenever possible, one obtains for $F_2^{\gamma(P^2)}$ [10, 11]

$$\frac{1}{x}F_{2,QPM}^{\gamma(P^2)}(x,Q^2) = 3\sum_q e_q^4 \frac{\alpha}{\pi}\left\{ \left[x^2+(1-x)^2\right]\left(\ln\frac{Q^2}{P^2}+\ln\frac{1}{x^2}\right) - 2 + 6x - 6x^2\right\} \ . \quad (3)$$

It is important to notice that (3) is *different* from the result for on-shell ($P^2 = 0$) photons [19], due to the different regularization adopted here[2]. This difference will be relevant also for the formulation of a model for the parton content of virtual photons, since it is part of the perturbatively calculable boundary condition in NLO [10, 11].

The Q^2-evolutions of the photonic parton distributions are essentially the same for real and virtual transverse photons. The inhomogeneous evolution equations are most conveniently treated in the Mellin n moment space, where all convolutions simply factorize, and the solutions can be given analytically (see, e.g., [23, 13]). Let us only recall here that the distributions $f^{\gamma(P^2)}(x,Q^2)$, obtained from solving the inhomogeneous evolution equations, can be separated into a 'pointlike' (inhomogeneous) and a 'hadronic' (homogeneous) part

$$f^{\gamma(P^2),n}(Q^2) = f_{PL}^{\gamma(P^2),n}(Q^2) + f_{HAD}^{\gamma(P^2),n}(Q^2) \ . \quad (4)$$

In NLO the pointlike singlet solution is schematically given by [23, 13]

$$\vec{f}_{PL}^{\gamma(P^2),n} = \left(\frac{2\pi}{\alpha_s}+\hat{U}\right)\left(1-L^{1+\hat{d}}\right)\frac{1}{1+\hat{d}}\,\vec{a} + \left(1-L^{\hat{d}}\right)\frac{1}{\hat{d}}\,\vec{b} \ , \quad (5)$$

and the usual NLO hadronic solution can be found, e.g, in [23, 13]. $\vec{a}$, $\vec{b}$, $\hat{d}$, and $\hat{U}$ in (5) stand for certain combinations of the photon-parton splitting functions and the QCD β-function [23, 13], and $L \equiv \alpha_S(Q^2)/\alpha_s(Q_0^2)$.

Let us finish this technical part by quoting the relevant NLO expression for the structure function $F_2^{\gamma(P^2)}(x,Q^2)$. It should be pointed out that the treatment and expressions for $f^{\gamma(P^2)}(x,Q^2)$ (as *on-shell* transverse partons obeying the usual Q^2-evolution equations) presented above *dictates* an identification of the relevant resolved $f^{\gamma(P^2)}X \to X'$ sub-cross sections with that of the real photon according to $\hat{\sigma}^{f^{\gamma(P^2)}X\to X'} = \hat{\sigma}^{f^{\gamma}X\to X'}$. In particular, the calculation of $F_2^{\gamma(P^2)}(x,Q^2)$ requires the same hadronic Wilson coefficients $C_{2,q}$ and $C_{2,g}$ as for $P^2 = 0$,

$$F_2^{\gamma(P^2)} = \sum_{q=u,d,s} 2xe_q^2\left\{q^{\gamma(P^2)} + \frac{\alpha_s}{2\pi}\left(C_{2,q}*q^{\gamma(P^2)} + C_{2,g}*g^{\gamma(P^2)}\right) + \frac{\alpha}{2\pi}e_q^2 C_{2,\gamma}\right\} + F_{2,c}^{\gamma(P^2)} \ , \quad (6)$$

where $F_{2,c}^{\gamma(P^2)}$ represents the charm contribution (see Sec. 4) and $*$ denotes the usual Mellin convolution. Note that in the DIS$_\gamma$ scheme, the NLO direct photon contribution $C_{2,\gamma}$ in (6) is absorbed into the evolution of the photonic quark densities, i.e., $C_{\gamma,2} = 0$ [23]. The difference in the QPM expressions for $F_2^{\gamma(P^2)}$ between real and virtual photons (as pointed out below Eq. (3)), i.e., in the expressions for $C_{2,\gamma}$, is then accounted for by a perturbatively calculable boundary condition for $q^{\gamma(P^2)}$ in NLO [13]. The LO expression for $F_2^{\gamma(P^2)}$ is obviously entailed in (6) by dropping all $C_{i,\gamma}$. Finally, it should be noted that $F_2^{\gamma(P^2)}$ is kinematically constrained within [11] $0 \leq x \leq (1+P^2/Q^2)^{-1}$.

[2]Note that $F_L^{\gamma(P^2)}$ is independent of the regularization adopted for calculating $\gamma^*(Q^2)\gamma(P^2) \to q\bar{q}$.

3 Comparison of different theoretical models

Let us now briefly highlight the main features of the available theoretical models for the parton densities of virtual photons:

GRS (Glück, Reya, Stratmann) [13]: The GRS distributions provide a straightforward and simple extension of the phenomenologically successful GRV photon densities [24] to non-zero P^2 in LO *and* NLO. As for the GRV densities, the NLO boundary conditions are formulated in the DIS_γ factorization scheme, originally introduced for $P^2 = 0$ to overcome perturbative instability problems arising in the conventional $\overline{\mathrm{MS}}$ scheme for large values of x (see [23] for details). At the low input scale $Q_0 = \mu \simeq 0.5\,\mathrm{GeV}$, universal for all 'radiatively generated' GRV distributions (proton, pion, and photon), the parton densities of real photons are solely given by a simple VMD-inspired input in LO and NLO(DIS_γ). All one needs to fully specify the distributions for $P^2 \neq 0$ is a simple, physically reasonable prescription which smoothly interpolates between $P^2 = 0$ (region (I)) and $P^2 \gg \Lambda^2_{QCD}$ (region (III)). This may be fixed by [13]

$$f^{\gamma(P^2)}(x, Q^2 = \tilde{P}^2) = \eta(P^2) f^{\gamma(P^2)}_{non-pert}(x, \tilde{P}^2) + \left[1 - \eta(P^2)\right] f^{\gamma(P^2)}_{pert}(x, \tilde{P}^2) \tag{7}$$

with $\tilde{P}^2 = \max(P^2, \mu^2)$ and $\eta(P^2) = (1 + P^2/m_\rho^2)^{-2}$ where m_ρ refers to some effective mass in the vector-meson propagator. Note that the ansatz (7) implies that the input parton distributions are frozen at the input scale μ for real photons for $0 \leq P^2 \leq \mu^2$ such that the only P^2 dependence in region (II) stems from the dipole dampening factor $\eta(P^2)$. In NLO(DIS_γ) the perturbatively calculable input $f^{\gamma(P^2)}_{pert}(x, \tilde{P}^2)$ in Eq. (7) is determined by the QPM box result (3); in LO it vanishes (see [13] for details). Since almost nothing is known experimentally about the parton structure of vector mesons, the VMD-like non-perturbative input is simply taken to be proportional to the GRV pion densities f^π [25]

$$f^{\gamma(P^2)}_{non-pert}(x, \tilde{P}^2) = \kappa\,(4\pi\alpha/f_\rho^2) \times \begin{cases} f^\pi(x, P^2) & , \quad P^2 > \mu^2 \\ f^\pi(x, \mu^2) & , \quad 0 \leq P^2 \leq \mu^2 \end{cases} \tag{8}$$

where μ, κ, f_ρ are specified in [24].

The resulting u-quark and gluon distributions $u^{\gamma(P^2)}(x, Q^2)$ and $g^{\gamma(P^2)}(x, Q^2)$, respectively, are shown in Fig. 1 for $Q^2 = 10\,\mathrm{GeV}^2$ and some representative values of P^2. With $g^{\gamma(P^2)}$ being the same in the DIS_γ and $\overline{\mathrm{MS}}$ scheme, the shown DIS_γ results for $u^{\gamma(P^2)}$ can be easily transformed to the conventional $\overline{\mathrm{MS}}$ scheme [23, 24, 13]. As can be inferred from the purely perturbative ($\eta \equiv 0$) contributions, the non-perturbative components, entering for $\eta \neq 0$ in Eq. (7), are non-negligible and partly even dominant (especially for $x \lesssim 0.01$). It turns out [13] that only for unexpectedly large $P^2 \gg m_\rho^2$, say, $P^2 (\ll Q^2)$ larger than about $10\,\mathrm{GeV}^2$, the perturbative component starts to dominate over the entire x range shown (cf., e.g., Fig. 13 in [13] for $P^2 = 20,\, 100\,\mathrm{GeV}^2$ and $Q^2 = 1000\,\mathrm{GeV}^2$).

The precise form of $\eta(P^2)$ in Eq. (7) clearly represents, apart from $f^{\gamma(P^2)}_{non-pert}$ itself, the largest uncertainty in this model and has to be tested by future experiments. The only measurement of the virtual photon structure in $\gamma^*(Q^2)\gamma(P^2)$ DIS available thus far [26], is compared in Fig. 2 with the NLO GRS prediction for $F^{\gamma(P^2)}_{eff} \equiv F_2 + \frac{3}{2}F_L$, the combination measured effectively by PLUTO [26] (see also Sec. 5). Due to the poor statistics of the data and the rather limited x range, the resummed NLO result cannot be distinguished from the naive, not resummed QPM result (dotted curve).

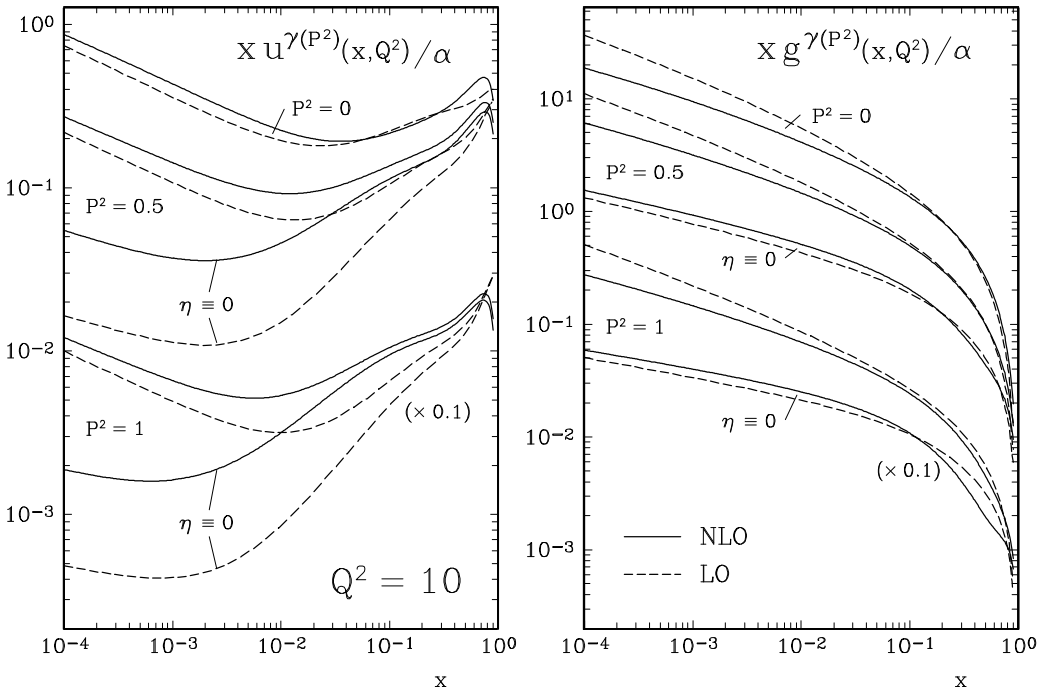

Figure 1: GRS [13] LO and NLO(DIS_γ) predictions for the u-quark and gluon content of a virtual photon for $Q^2 = 10\,\mathrm{GeV}^2$ and various fixed values of $P^2(\mathrm{GeV}^2)$. For comparison, the LO and NLO GRV parton distributions of the real photon $(P^2 = 0)$ [24] are shown as well.

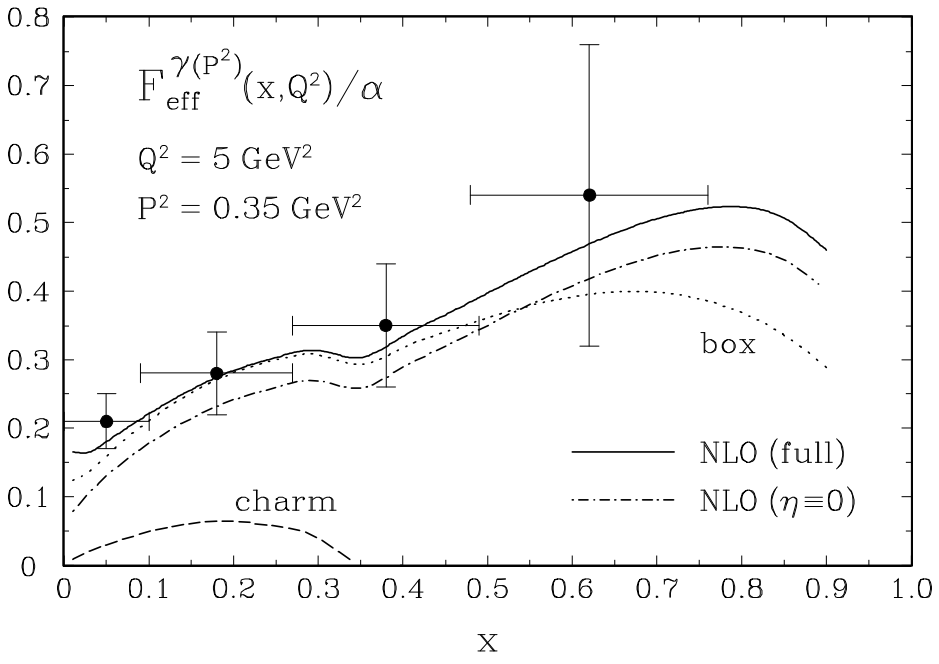

Figure 2: NLO GRS predictions for $F_{eff}^{\gamma(P^2)} \equiv F_2 + \frac{3}{2}F_L$ [13]. The data points are taken from PLUTO [26]. The purely perturbative results correspond to $\eta \equiv 0$ in Eq. (7).

Finally, it should be noted that in the GRS approach heavy quarks do not take part in the Q^2-evolution, i.e., there is *no* 'massless' photonic charm distribution [13]. Heavy flavors can only be produced *extrinsically*, and their contributions have to be calculated according to the appropriate massive sub-cross sections (see also Sec. 4). The LO GRS distributions are available in parametrized form for $P^2 < 10\,\mathrm{GeV}^2$ and $Q^2 \gtrsim 5P^2$ [5].

SaS (Schuler and Sjöstrand) [14, 15]: The starting point for their analysis are also some well-established LO sets of parton densities for real photons [14], SaS 1D and SaS 2D, corresponding to two rather different assumptions about the non-perturbative hadronic input[3]. The SaS 1D set has a similarly low input scale $Q_0 \simeq 0.6\,\mathrm{GeV}$ as in the GRV [24] and GRS [13] analyses, but instead of simply relating the VMD input distributions to that of a pion, a fit is performed to the coherent sum of the lowest-lying vector meson states ρ, ω, ϕ. For the SaS 2D set a 'conventional' high input scale $Q_0 = 2\,\mathrm{GeV}$ is used at the expense of two additional fit parameters, one characterizing the necessary additional 'hard' component for the quark input at larger values of Q_0, the other models the effect of additional vector meson states beside the ones already taken into account in the SaS 1D set. The shape of the SaS gluon densities are entirely fixed by theoretical estimates, no direct or indirect constraints from direct-photon production data in πp collisions as in the GRV analysis [24] have been imposed. Contrary to GRS, heavy flavors are included as massless partons in the photon above the threshold $Q^2 > m_q^2$, but when calculating/fitting the available $F_2^\gamma(x, Q^2)$ data, the massive 'Bethe-Heitler' cross section for $\gamma^*\gamma \to c\bar{c}$ is used instead, which is, however, not entirely consistent due to double counting.

The extension to non-zero P^2 is based on the fact that the n moments of the photon densities parton can be expressed as a dispersion-integral in the mass k^2 of the $\gamma \to q\bar{q}$ fluctuations, which links perturbative and non-perturbative contributions [14, 15]. Having assumed some model-dependent weight function for the dispersion-integral, and after associating the low-k^2 part with some discrete set of vector mesons (as for $P^2 = 0$), one arrives at their final expression for the parton densities of virtual photons [14, 15]

$$f^{\gamma(P^2)}(x, Q^2) = \sum_V \frac{4\pi\alpha}{f_V^2} \left[\frac{m_V^2}{m_V^2 + P^2}\right]^2 f^{\gamma,V}(x, Q^2, \tilde{P}^2) + \sum_q \frac{\alpha}{\pi} e_q^2 \int_{\tilde{P}^2}^{Q^2} \frac{dk^2}{k^2} f^{\gamma\to q\bar{q}}(x, Q^2, k^2)\ , \tag{9}$$

where in the perturbative contribution the suppression factor $[k^2/(k^2 + P^2)]^2$ has been substituted by an effective lower cut-off $\tilde{P}^2$ for the integration. Both components $f^{\gamma,V}$ and $f^{\gamma\to q\bar{q}}$ in (9) integrate to unit momentum. As in the GRS model above, the VMD part contains a dipole suppression factor, which dampens all non-perturbative contributions with increasing virtuality P^2. Contrary the the GRS approach, several different choices for the input scale $\tilde{P}^2$ have been studied apart from $\tilde{P}^2 = \max(Q_0^2, P^2)$ [15]. The differences between all these procedures can be viewed as a measure for the theoretical uncertainty within this approach (see, e.g., Figs. 1 and 2 in [15]). It should be also noted that for some more complicated choices for $\tilde{P}^2$, the photonic parton densities obey evolution equations different from those of the real photon, e.g., the inhomogeneous term can be modified by a factor $Q^2/(Q^2 + P^2)$ [15]. All different sets of distributions are available in parametrized form [14, 15] but, for the time being, the SaS analysis is restricted to LO only.

Fig. 3 compares the LO GRS with the LO SaS 1D and SaS 2D distributions (choosing $\tilde{P}^2 = \max(Q_0^2, P^2)$) for $Q^2 = 10\,\mathrm{GeV}^2$ and two P^2 values relevant for future LEP2 measurements [27]. As can be seen, the SaS 1D results, which refer to a equally low input scale as used in GRS, and the GRS densities are rather similar, at least for the u-quark, whereas the SaS 2D (quark) distributions are sizeably smaller in this kinematical range, mainly due to the higher input scale. For smaller values of x (not shown in Fig. 3) the GRS densities rise more strongly than the SaS densities, due the different non-perturbative

[3]The additional SaS 1M and SaS 2M sets [14] are theoretically inconsistent, as the LO evolved densities are combined with the NLO scheme-dependent photon-coefficient function $C_{2,\gamma}$ in the calculation of F_2^γ in LO. These sets should not be used in phenomenological analyses.

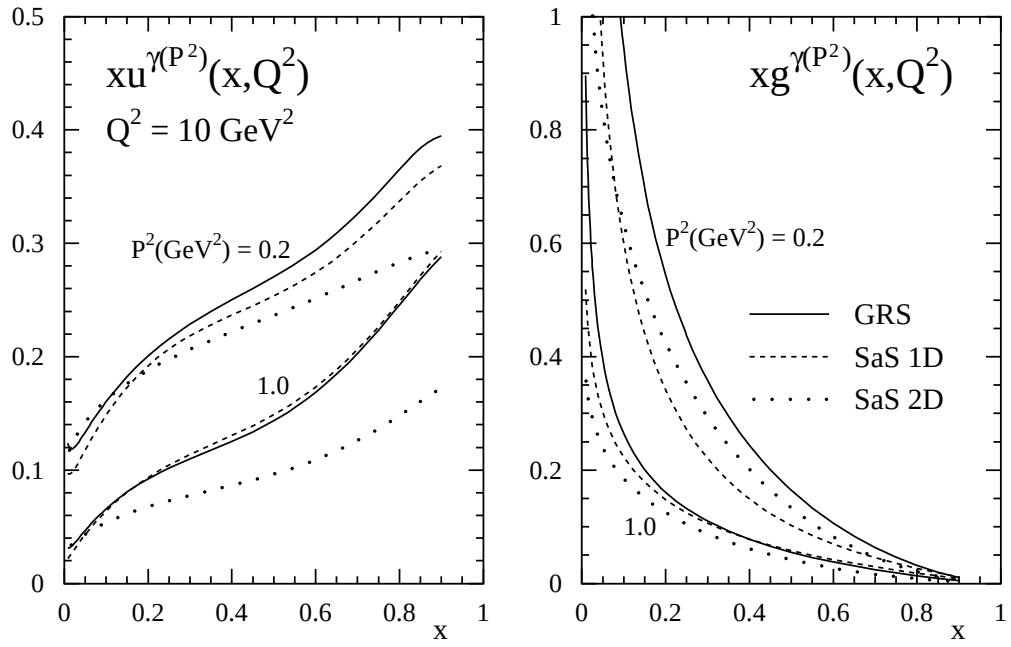

Figure 3: Comparison of the LO GRS predictions [13] for the u-quark and gluon content of virtual photons with the SaS 1D and SaS 2D results for $\tilde{P}^2 = \max(Q_0^2, P^2)$ [14] at $Q^2 = 10\,\mathrm{GeV}^2$ and for two values of P^2.

input. However, with increasing P^2 all differences get, of course, more or less washed out, since one approaches the purely perturbative domain and the differences in the treatment of the non-perturbative component become negligible.

DG (Drees and Godbole) [16]: The aim of this analysis is to estimate the influence of the high-P^2 tail in the photon flux in untagged or anti-tagged events, i.e., to study the impact of virtual photons in a sample of almost real photons. This effect should be taken into account if one tries to extract the parton densities of real photons from such measurements. To perform a quantitative analysis, DG provide a simple interpolating multiplicative factor r which can be applied to *any* set of distributions of real photons. Several different forms for r are studied in [16], and one of the main alternatives is

$$r = 1 - \frac{\ln(1 + P^2/P_c^2)}{\ln(1 + Q^2/P_c^2)} \ , \tag{10}$$

where P_c denotes some typical hadronic scale like, for instance, the ρ mass. The factor r is applied to all quark flavors, but the gluon is expected to be further suppressed, since it is radiated off the quarks [12]:

$$q^{\gamma(P^2)}(x, Q^2) = r q^{\gamma}(x, Q^2) \ , \ g^{\gamma(P^2)}(x, Q^2) = r^2 g^{\gamma}(x, Q^2) \ . \tag{11}$$

For typical $\gamma\gamma$ experiments with $Q^2 \simeq 10\,\mathrm{GeV}^2$ in an untagged situation, virtual photon effects then suppress the effective photonic quark and gluon content by about 10 and 15%, respectively [16].

Obviously, the above ansatz (11) does not change the x shape of the distributions, which would require more complicated forms for r [16]. The recipe (11) does not appear to be well suited for QCD tests of the virtual photon content: on the one hand the densities in (11) are not a solution of the inhomogeneous evolution equations, and on the other hand there is no dipole power suppression factor for the non-perturbative VMD part of

the virtual photon densities as in GRS [13] or SaS [14, 15], i.e., the approximation (11) can only be applied in the large x region where the perturbative pointlike part dominates, whereas at smaller x it may grossly overestimates the densities for increasing virtuality P^2. A similar strategy as in Eqs. (10) and (11) has been used in [18] including, however, a power suppressed VMD part.

4 Treatment of heavy flavors

The question of how to treat heavy flavor ($m_q \gg \Lambda_{QCD}$) contributions to structure functions and cross sections in the most appropriate and reliable way has attracted a considerable amount of interest in the past few years [21, 22, 28]. This was mainly triggered by the observation that the charm contribution to the DIS proton structure function F_2^p amounts to about $20-25\%$ in the small x region covered by HERA. In case of the photon structure function $F_2^{\gamma(P^2)}$ in (6), effects due to charm are sizeable also in the large x region due to the existence of the direct/pointlike component, such that a proper treatment is even more important here.

There are two extreme ways to handle heavy flavors: one can simply include heavy flavors as massless partons in the evolution above some threshold $Q^2 \gtrsim m_q^2$, or one can stick to a picture with only light partons in the proton/photon. In the latter case, heavy flavors do not participate in the evolution equations at all and can be produced only extrinsically. In case of $F_{2,c}^{\gamma(P^2)}$ in (6), two different contributions have to be taken into account. Firstly, the direct 'Bethe-Heitler' process $\gamma^*(Q^2)\gamma(P^2) \to c\bar{c}$, and secondly the resolved contribution $\gamma^*(Q^2)g^{\gamma(P^2)} \to c\bar{c}$. For real photons these cross sections are known up to NLO and can be found in [29]. In [30] it was shown that the two contributions are separated in the variable x: for large x, say, $x \gtrsim 0.05$, the direct process dominates, whereas for $x \lesssim 0.01$ the dominant contribution stems from the resolved part.

The fully massless treatment has been abandoned recently in all existing modern sets of proton densities, simply because it does not exhibits the correct x *and* Q^2 dependent threshold behavior. A potential problem with the massive treatment are possibly large logarithms in the relevant sub-cross sections far above the threshold, which *might* be indicative for resummations, i.e., for introducing a 'massless' heavy quark distribution. Therefore various 'unified' prescription were proposed recently [22] which reduce to the massive results close to, and to the massless picture far above threshold. For the time being these studies have been performed only for the proton densities and not in the context of photons.

However, as mentioned in Sec. 3, GRS [13] prefer to stick to the fully massive framework, similarly to the case of the GRV proton densities [31]. In each case this is motivated by the observation that all relevant fully massive production mechanisms appear to be perturbatively stable, at least for all experimentally relevant values of x and Q^2 (see, e.g., Refs. [21, 30]). Moreover, all theoretical uncertainties, in particular the dependence on the factorization scale appear to be well under control, leading to the conclusion that there is no real need for any resummation procedure. It should be mentioned that the relevant expressions for $\gamma^*(Q^2)\gamma(P^2) \to c\bar{c}$ for non-zero P^2 are available only in LO so far [32], hence a study of the perturbative stability cannot be performed here yet.

Clearly, the fully massive treatment is much more cumbersome and inconvenient than the massless or 'unified' framework when calculating, for instance, jet production cross sections in ep or $\gamma\gamma$ collisions. One cannot simply increase the number of active flavors by

one unit and use a $c^{\gamma(P^2)}(x,Q^2)$ distribution. Instead one has to calculate the relevant subcross sections with massive quarks for the final state configuration under consideration, which is much more involved and time-consuming in numerical analyses. However, for large-p_T jet production in LO ($m_q/p_T \ll 1$), for instance, one can simply approximate the relevant massive cross sections by their massless counterparts, neglecting of course all massless contributions with a 'heavy' quark in the initial state.

5 Measuring γ^*-PDF's in e^+e^- and ep reactions

Since there are several dedicated contributions which discuss recent experimental progress or future prospects [4, 7, 33], we can be fairly brief here and concentrate only on topics not covered elsewhere.

Let us first of all delineate the x, Q^2, and P^2 ranges covered by LEP2 and the expected statistical accuracy for the virtual photon structure functions measurements [27]. Because of its higher energy and integrated luminosity, LEP2 can provide improved information from double tagged events as compared to the not very precise results from PLUTO [26] shown in Fig. 2. The most important double tag sample at LEP2 is expected to come from events with $Q^2 \gtrsim 3\,\mathrm{GeV}^2$ and $0.1 \lesssim P^2 \lesssim 1\,\mathrm{GeV}^2$. For typically expected $500\,\mathrm{pb}^{-1}$ of data collected, about 800 of such events will be seen, covering $3 \cdot 10^{-4} \lesssim x < 1$ and $3 \lesssim Q^2 \lesssim 1000\,\mathrm{GeV}^2$ [27]. The yield of events with both Q^2 and $P^2 \gtrsim 3\,\mathrm{GeV}^2$ seems to be too small for a meaningful analysis.

Fig. 4 shows the virtual photon structure function $F_2^{\gamma(P^2)}(x,Q^2)$ in LO as predicted by the SaS 1D, SaS 2D (using $\tilde{P}^2 = \max(Q^2,P^2)$), and GRS models in two bins for P^2 and Q^2. The error bars indicate the statistical precision expected for each x bin using the SaS 1D densities (similar for the SaS 2D and GRS distributions). A measurement of $F_2^{\gamma(P^2)}(x,Q^2)$ within these bins, as distinct from the real ($P^2 = 0$) photon structure function (illustrated by the solid curves for SaS 1D) should be possible at LEP2 and could be compared to the different model predictions, which turn out to be rather similar in the accessible x, Q^2, and P^2 bins, except for the smallest x bins and $P^2 \to 0$ ($\langle P^2 \rangle = 0.2\,\mathrm{GeV}^2$). The latter differences are of course related to the present ignorance of the $P^2 = 0$ distributions for $x \to 0$, i.e., whether they either steeply rise as in case of GRV [24] or show a rather flat $x \to 0$ behaviour as, e.g., in case of SaS 2D [14, 15].

However, apart from the experimental challenge there is an additional complication already noticed by PLUTO [26]: what is directly measured is, of course, *not* $F_2^{\gamma(P^2)}$ but the $\gamma^*(Q^2)\gamma(P^2)$ DIS cross section, which can be schematically expanded as $\sigma_{\gamma^*(Q^2)\gamma(P^2)} = \sigma_{TT} + \varepsilon_1\sigma_{LT} + \varepsilon_2\sigma_{TL} + \varepsilon_1\varepsilon_2\sigma_{LL}$, where L and T denote longitudinal and transverse polarization, respectively, of the probe and the target photons, and $\varepsilon_{1,2}$ are the L/T γ-flux ratios. For PLUTO [26] $\varepsilon_1 \simeq \varepsilon_2 \simeq 1$ ($\Leftrightarrow y \ll 1$) and *assuming* that $\sigma_{LL} \simeq 0$ and $\sigma_{LT} = \sigma_{TL}$, as for the QPM expressions for $\gamma^*_{T,L}(Q^2)\gamma_{T,L}(P^2) \to q\bar{q}$ for vanishing constituent quark masses [32], one arrives at the combination [26] $\sigma_{\gamma^*\gamma} \sim F_2 + 3/2F_L \equiv F_{eff}^{\gamma(P^2)}$ effectively measured by PLUTO (cf. Fig. 2). Hence, strictly speaking such measurements cannot be directly related to the densities $f^{\gamma(P^2)}(x,Q^2)$, since only *transverse* (T) virtual photons are described by the GRS, SaS, and DG models. Furthermore, in the QPM model [32] it turns out that the contribution due to longitudinal target photons is rather sizeable at large x even for $P^2/Q^2 \ll 1$, contrary to the expectation that transverse photons should dominate in this region. Clearly, more work is required here for a meaningful interpretation of any future results from LEP2, possibly including also studies of the parton

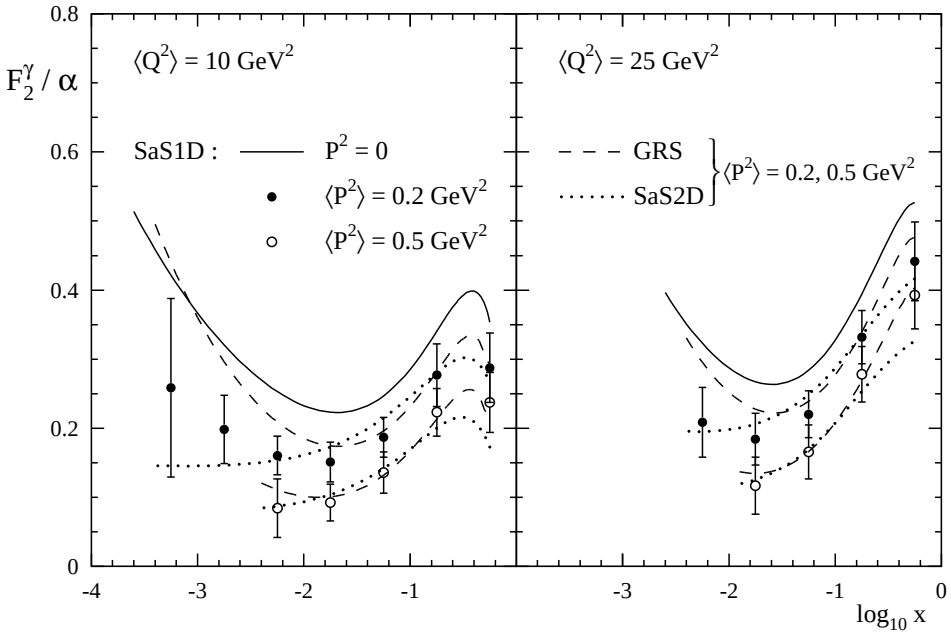

Figure 4: Expectations for the statistical accuracy of the virtual photon structure measurement at LEP2 in two different P^2 and Q^2 bins using the SaS 1D distributions [14]. The SaS 1D predictions for $P^2 = 0$ and the results for the GRS [13] and SaS 2D models are shown as lines for comparison. The upper (lower) curves for GRS and SaS 2D refer to $P^2 = 0.2\,(0.5)\,\mathrm{GeV}^2$, respectively. The figure is taken from [27].

content of longitudinal photons which have not been carried out so far.

In *ep* collisions (di-)jet production is certainly the best tool to decipher the parton structure of virtual photons, and a lot of experimental and theoretical progress was reported at the workshop [4, 7]. There should be a hierarchy between the hard scale μ_f^2 ($= Q^2$ in e^+e^-) at which the virtual photon is probed (typically $\mu_f^2 = \mathcal{O}(P^2 + p_{T,jet}^2)$ in case of jet production) and the photon virtuality P^2 (see footnote 1). Exactly in this kinematical domain an excess in the dijet rate was observed by H1 [4], which can be nicely attributed to a resolved virtual photon contribution, in accordance with all existing models for the $f^{\gamma(P^2)}$ described in Sec. 3.

Recently, similar studies were extended to the production rate of forward jets [33], which is regarded as a test in favor of the BFKL dynamics [34]. Indeed the usual DGLAP (direct photon induced) cross section falls short of the data by roughly a factor of two [35]. In [33] it was demonstrated, however, that the inclusion of the resolved virtual photon component removes this discrepancy, and the full DGLAP results are then in even better agreement with data than the BFKL results, in particular for the two to one forward jet ratio [35]. However one should be cautious to jump to any conclusions. In order to suppress the phase space for the DGLAP evolution, the p_T^2 of the forward jet is required to be of the same size as the virtuality P^2 of the photon, hence there is no real hierarchy between the hard scale $\mu_f^2 = \mathcal{O}(P^2 + p_{T,jet}^2)$ and P^2 and thus no large logarithm $\ln \mu_f^2/P^2$ which is resummed in $f^{\gamma(P^2)}$. Naively one would therefore expect only a small resolved contribution, as was also observed in the H1 jet analysis [4] or in the theoretical studies [7] for $P^2 \to \mu_f^2$, rather than a gain by about a factor of two. Hence the kinematics of forward jets seems to be very subtle (for instance, the virtual photon content is only probed at large momentum fractions x_γ), and presumably the theoretical uncertainties due to scale variations and changes in the model for the $f^{\gamma(P^2)}$ (in particular, of the input scale $\tilde{P}^2$)

are of the same size as the resolved photon contribution itself. More detailed studies are clearly required here. Furthermore, it should be kept in mind that all BFKL results so far are based only LO parton level calculations. It seems, however, that the forward jet kinematics is not suited to distinguish between BFKL and DGLAP at HERA [33].

References

[1] E. Witten, Nucl. Phys. **B120** (1977) 189.

[2] Recent experimental results can be found in, e.g., the proc. of the 'Photon '97 Conference', Egmond aan Zee, 1997, A. Buijs and F.C. Erne (eds.); see also the contributions by M. Kienzle, B. Surrow, I. Tyapkin, and Y. Yamazaki in these proceedings.

[3] M.L. Utley, in proc. of the 'Europhysics Conference (HEP'95)', Brussels, 1995, J. Lemonne et al. (eds.), World Scientific, p. 570;
C. Adloff et al., H1 collab., Phys. Lett. **B415** (1997) 418; `hep-ex/9806029`.

[4] S. Maxfield, these proceedings.

[5] M. Glück, E. Reya, and M. Stratmann, Phys. Rev. **D54** (1996) 5515.

[6] D. de Florian, C. Garcia Canal, and R. Sassot, Z. Phys. **C75** (1997) 265;
J. Chyla and J. Cvach, in proc. of the 1995/96 workshop on 'Future Physics at HERA', DESY, G. Ingelman et al. (eds.), p. 545; in proc. of 'Photon '97 Conference', Egmond aan Zee, 1997, A. Buijs and F.C. Erne (eds.).

[7] M. Klasen, G. Kramer, and B. Pötter, Eur. Phys. J. **C1** (1998) 261;
G. Kramer and B. Pötter, Eur. Phys. J. **C5** (1998) 665;
B. Pötter, these proceedings.

[8] B. Pötter, `hep-ph/9806437`.

[9] H. Jung, Comp. Phys. Comm. **86** (1995) 147.

[10] T. Uematsu and T.F. Walsh, Phys. Lett. **101B** (1981) 263, Nucl. Phys. **B199** (1982) 93.

[11] G. Rossi, Phys. Rev. **D29** (1984) 852; UC San Diego report UCSD-10P10-227 (unpublished).

[12] F.M. Borzumati and G.A. Schuler, Z. Phys. **C58** (1993) 139.

[13] M. Glück, E. Reya, and M. Stratmann, Phys. Rev. **D51** (1995) 3220.

[14] G.A. Schuler and T. Sjöstrand, Z. Phys. **C68** (1995) 607.

[15] G.A. Schuler and T. Sjöstrand, Phys. Lett. **B376** (1996) 193.

[16] M. Drees and R.M. Godbole, Phys. Rev. **D50** (1994) 3124.

[17] C.F. von Weizsäcker, Z. Phys. **88** (1934) 612;
E.J. Williams, Phys. Rev. **45** (1934) 729;
S. Frixione, M.L. Mangano, P. Nason, and G. Ridolfi, Phys. Lett. **B319** (1993) 339.

[18] P. Aurenche et al., Prog. Theor. Phys. **92** (1994) 175; in proc. of the workshop on 'Two-Photon Physics at LEP and HERA', Lund, 1994, G. Jarlskog and L. Jönsson (eds.), p. 269.

[19] T.F. Walsh and P.M. Zerwas, Phys. Lett. **44B** (1973) 195.

[20] W.A. Bardeen and A.J. Buras, Phys. Rev. **D20** (1979) 166; **D21** (1980) 2041(E).

[21] M. Glück, E. Reya, and M. Stratmann, Nucl. Phys. **B422** (1994) 37.

[22] M. Aivazis, F. Olness, and W.-K. Tung, Phys. Rev. **D50** (1994) 3085;
M. Aivazis, J.C. Collins, F. Olness, and W.-K. Tung, Phys. Rev. **D50** (1994) 3102;
A.D. Martin, R.G. Roberts, M.G. Ryskin, and W.J. Stirling, Eur. Phys. J. **C2** (1998) 287;
R.S. Thorne and R.G. Roberts, Phys. Rev. **D57** (1998) 6781; Phys. Lett. **B421** (1998) 303;
M. Buza, Y. Matiounine, J. Smith, and W.L. van Neerven, Phys. Lett. **B411** (1997) 211; Eur. Phys. J. **C1** (1998) 301.

[23] M. Glück, E. Reya, and A. Vogt, Phys. Rev. **D45** (1992) 3986.

[24] M. Glück, E. Reya, and A. Vogt, Phys. Rev. **D46** (1992) 1973.

[25] M. Glück, E. Reya, and A. Vogt, Z. Phys. **C53** (1992) 651.

[26] Ch. Berger et al., PLUTO collab., Phys. Lett. **142B** (1984) 119.

[27] '$\gamma\gamma$ Physics' working group report, P. Aurenche and G.A. Schuler (conv.), CERN 96-01, vol. 1, p. 291.

[28] M. Drees and R.M. Godbole, in proc. of the 'Photon '95 Conference', Sheffield, 1995, D.J. Miller et al. (eds.), World Scientific, p. 123.

[29] E. Laenen, S. Riemersma, J. Smith, and W.L. van Neerven, Phys. Rev. **D49** (1994) 5753.

[30] E. Laenen and S. Riemersma, Phys. Lett. **B376** (1996) 169.

[31] M. Glück, E. Reya, and A. Vogt, Z. Phys. **C67** (1995) 433; Eur. Phys. J. **C5** (1998) 461.

[32] V.M. Budnev, I.F. Ginzburg, G.V. Meledin, and V.G. Serbo, Phys. Rep. **15** (1975) 181.

[33] H. Jung, L. Jönsson, and H. Küster, `hep-ph/9805396`;
H. Jung, these proceedings.

[34] A.H. Mueller, Nucl. Phys. Proc. Suppl. **18C** (1990) 125; J. Phys. **G17** (1991) 1443.

[35] J. Breitweg et al., ZEUS collab., `hep-ex/9805016` (Eur. Phys. J. **C**);
C. Adloff et al., H1 collab., `hep-ex/9809028`.